

THE MORPHOLOGY OF PASSIVELY EVOLVING GALAXIES AT $Z \sim 2$ FROM *HST*/WFC3 DEEP IMAGING IN THE HUBBLE ULTRADEEP FIELD¹

P. CASSATA², M. GIAVALISCO², YICHENG GUO², H. FERGUSON³, A. KOEKEMOER³, A. RENZINI⁴, A. FONTANA⁵, S. SALIMBENI², M. DICKINSON⁶, S. CASERTANO³, C. J. CONSELICE⁷, N. GROGIN³, J. M. LOTZ⁶, C. PAPOVICH⁸, R. A. LUCAS³, A. STRAUGHN⁹, JONATHAN. P. GARDNER⁹, L. MOUSTAKAS¹⁰

Draft version October 29, 2018

ABSTRACT

We present near-IR images, obtained with the *Hubble Space Telescope* (*HST*) and the WFC3/IR camera, of six passive and massive galaxies at redshift $1.3 < z < 2.4$ ($\text{SSFR} < 10^{-2} \text{ Gyr}^{-1}$; stellar mass $M \sim 10^{11} M_{\odot}$), selected from the Great Observatories Origins Deep Survey (GOODS). These images, which have a spatial resolution of $\sim 1.5 \text{ kpc}$, provide the deepest view of the optical rest-frame morphology of such systems to date. We find that the light profile of these galaxies is regular and well described by a Sérsic model with index typical of today's spheroids. Their size, however, is generally much smaller than today's early types of similar stellar mass, with four out of six galaxies having $r_e \sim 1 \text{ kpc}$ or less, in quantitative agreement with previous similar measures made at rest-frame UV wavelengths. The images reach limiting surface brightness $\mu \sim 26.5 \text{ mag arcsec}^{-2}$ in the F160W bandpass; yet, there is no evidence of a faint halo in the galaxies of our sample, even in their stacked image. We also find that these galaxies have very weak “morphological k-correction” between the rest-frame UV (from the ACS z -band), and the rest-frame optical (WFC3 H -band): the Sérsic index, physical size and overall morphology are independent or only mildly dependent on the wavelength, within the errors.

Subject headings: cosmology: observations — galaxies: fundamental parameters — galaxies: evolution

1. INTRODUCTION

Most of the stars observed in today's early-type galaxies have formed at high redshifts ($z > 2$, see Renzini 2006), but the observations have not yet constrained how that stellar mass has assembled in the presently observed systems.

Several groups have reported that at least in the range $M > M \sim 10^{11} M_{\odot}$, the stellar mass function of these high-redshift “elliptical galaxies”, appears to be rapidly increasing from $z \sim 3$ to $z \sim 1$, pointing to this epoch as one of major assembly for modern bright galaxies (e.g. Bundy et al. 2006; Fontana et al. 2006; Arnouts et al. 2007; Scarlata et al. 2007; Ilbert et al. 2009). A number of mechanisms have been proposed as drivers of this evolution,

from merging to gradual in-situ accretion (Naab et al. 2009; van Dokkum et al. 2009; Hopkins et al. 2010).

Elliptical galaxies at $z > 1.5$ are often observed to be smaller, by factors $\sim 3 - 5\times$, than their local counterparts of similar stellar mass, and thus to have $\approx 30 - 100\times$ higher stellar density (Daddi et al. 2005; Trujillo et al. 2006; Trujillo et al. 2007; Toft et al. 2007; Zirm et al. 2007; Longhetti et al. 2007; Cimatti et al. 2008, Van Dokkum et. al. 2008, Buitrago et al. 2008, Toft et al. 2009), a fact that still lacks an explanation in terms of an evolutionary mechanism.

Some have suggested that current observations at high redshift could have missed low surface-brightness halos surrounding the galaxies, due to the relatively limited sensitivity combined with the $(1+z)^4$ cosmological dimming (Hopkins et al. 2009b; Mancini et al. 2009). Others have proposed that surveys of the local universe (e.g. the SDSS, Stoughton et al. 2002) could have missed a relatively large fraction of very compact, yet massive early-type galaxies due to the limited ground-based angular resolution ($1''$ corresponds to a physical scale of $\sim 1 \text{ kpc}$ at $z = 0.05$). While recent works (Valentinuzzi et al. 2009; Trujillo et al. 2009) reported the identification of dense and massive galaxies in the local universe, their spatial abundance appears much smaller than the $z \sim 2$ galaxies.

Furthermore, while small high-redshift samples have been imaged with *HST* and NICMOS at rest-frame optical wavelengths (Buitrago et al. 2008; Trujillo et al. 2007; Toft et al. 2007; Zirm et al. 2007; Longhetti et al. 2007; Van Dokkum et. al. 2008), most of the galaxies have only been observed in the rest-frame UV with ACS, and the dependence of the morphology of these galax-

¹ Based on observations made with the NASA/ESA *Hubble Space Telescope* operated by the Association of Universities for Research in Astronomy (AURA), Inc., under contract NAS5-26555.

² Department of Astronomy, University of Massachusetts, Amherst, MA 01003; paolo@astro.umass.edu

³ Space Telescope Science Institute, 3700 San Martin Drive, Baltimore, MD, 21218

⁴ Osservatorio Astronomico di Padova (INAF-OAPD), Vicolo dell'Osservatorio 5, I-35122, Padova, Italy

⁵ INAF - Osservatorio Astronomico di Roma, via Frascati 33, Monteporzio-Catone (Roma), I-00040, Italy

⁶ NAO-Tucson, 950 North Cherry Avenue, Tucson, AZ 85719

⁷ University of Nottingham, School of Physics and Astronomy, Nottingham NG7 2RD

⁸ George P. and Cynthia Woods Mitchell Institute for Fundamental Physics and Astronomy, Department of Physics, Texas A&M University, College Station, TX 77843-4242, USA

⁹ Astrophysics Science Division, Observational Cosmology Laboratory, Goddard Space Flight Center, Code 665, Greenbelt, MD 20771

¹⁰ Jet Propulsion Laboratory, California Institute of Technology, MS 169-327, Pasadena, CA 91109

ies on the wavelength has not been characterized (Cimatti et al. 2008; Daddi et al. 2005).

In this letter we use the unprecedented sensitivity and angular resolution of WFC3/IR images recently acquired in the HUDF to study the optical rest-frame morphology of a small but well defined sample of low SSFR galaxies at $z \sim 2$. AB magnitudes are used throughout this paper, and, when needed, a Λ -CDM world model with $H_0 = 70$ km s $^{-1}$ Mpc $^{-1}$, $\Omega_M = 0.3$ and $\Omega_\Lambda = 0.7$.

2. DATA REDUCTION, SAMPLE SELECTION AND MORPHOLOGICAL ANALYSIS

The primary imaging data consist of the first epoch of WFC3/IR observations acquired by Illingworth et al. (2009, program ID=GO11563) in the HUDF (Beckwith et al. 2006), and thus the field is fully embedded in the GOODS-South field (Giavalisco et al. 2004). The images have been acquired in the F105 (Y), F125W (J) and F160W (H) filters and covers an area roughly equal to the footprint of the WFC3/IR camera (2.1 arcmin 2). We have carried out our independent reduction of the raw data and after rejecting images affected by persistence in the J -band, our final stacks reach $1 - \sigma$ surface brightness fluctuations of 27.2, 26.6 and 26.3 AB/arcsec 2 in the three bands, respectively. We have drizzled the WFC3 images to 0.06" pixel scale and brought them into registration with the HUDF ACS and GOODS ones. The size of the PSF of the stacks is 0.18" in the H-band. We have then created a multi-wavelength source catalog (GUTFIT, Grand Unified TFIT Catalog) using the TFIT procedures by Laidler et al. (2007), which contains PSF-matched photometry in all the bands acquired by the GOODS multi-facility program, from the U to the 8 μ m IRAC one.

We have selected a sample of high redshift, massive and passive galaxies using both the BzK color selection by Daddi et al. (2004), as well as multi-band SED fitting to spectral population synthesis models. While the BzK technique provides a well characterized criterion to select relatively massive galaxies with low specific star-formation rate at $1.4 < z < 2.5$, the method naturally has finite completeness and contamination. Thus, given the overall limited size of the sample, we have augmented it with galaxies at $z > 1.3$ selected for being massive and passive according the criteria $M > 10^{10} M_\odot$ and $SSFR < 10^{-2}$ Gyr $^{-1}$ based on fitting their observed broad-band SEDs to the Charlot & Bruzual (2007) and Maraston (2005) models. We have used Salpeter IMF and lower and upper mass limits 0.1 and 100 M_\odot , respectively, obtaining essentially identical results with both libraries. We have adopted the Calzetti et al. (2000) obscuration law to account for the possible (modest) presence of dust. Finally, all our sample galaxies have no detection at 24 μ m down to a $1 - \sigma$ limit of 5 μ Jy, consistent with predictions for passively evolving galaxies at $z \sim 2$ (Fontana et al. 2009).

The final sample consists of six galaxies, four of which have spectroscopic redshifts, namely # 22704 and # 23555 from Cimatti et al. (2008), # 24279 from Daddi et al. (2005) and # 24626 from Vanzella et al. (2008), and two for which we derived accurate ($\Delta z / (1 + z) \sim 0.05$) photometric redshifts from the GUTFIT multi-band photometry. Four out of six galaxies satisfy the pBzK criterion. Table 1 lists the sample,

including the parameters of the stellar populations from the fitted procedure, while Figure 1 shows the observed (points) and best-fit (curves) SED together with the H-band images of the galaxies.

We have used the GALFIT package (Peng et al. 2002) to fit the light profile of the galaxies in the z -, Y -, J - and H - bands to the Sérsic model

$$I(r) = I_e \exp \left\{ -b_n \left[\left(\frac{r}{r_e} \right)^{1/n} - 1 \right] \right\}, \quad (1)$$

where $I(r)$ is the surface brightness measured at distance r , I_e is the surface brightness at the effective radius r_e and b_n is a parameter related to the Sérsic index n . For $n=1$ and $n=4$ the Sérsic profile reduces respectively to an exponential or deVaucouleurs profile. Bulge dominated objects typically have high n values (e.g. $n > 2$) and disk dominated objects have n around unity. Cassata et al. (2005), Ravindranath et al. (2006) and Cimatti et al. (2008) showed that GALFIT yields unbiased estimates of the Sérsic index and effective radius.

We have obtained the PSF in each passband for use with GALFIT by averaging six well-exposed, unsaturated stars in the UDF/WFC3 field. For all galaxies, we ran multiple fits with the sky either set to a fixed, pre-established value or left as a free parameter. We also experimented with the size of the fitting region around each galaxy, finding peak-to-peak variations of the Sérsic indices and r_e at the 20% level at the most. The fits in Table 1 use a 6×6 arcsec 2 fitting region and free sky.

3. THE MORPHOLOGICAL PROPERTIES OF GALAXIES AT $Z \sim 2$.

Figure 2 shows the residual images obtained by subtracting the GALFIT best-fit models (after convolution with the PSF) from the corresponding images, together with the observed and best-fit model light profiles (see Table 1). All galaxies, except # 24646, are very compact and symmetric, in close resemblance to present-day spheroidal galaxies. Galaxy # 24626, the most extended of our sample, has isophotes that deviate from the elliptical shape, and the position angle of the isophotes varies as a function of the distance along the semi-major axis. These irregularities can be the result of ongoing or recent interactions (see Kormendy et al. 2009 and references therein).

Of the six galaxies, four have Sérsic index $\gtrsim 2$ (# 19389, # 22704, # 23555 and # 24626). In the case of object # 19389 we had to add a central unresolved (PSF) component to the Sérsic model to obtain a reasonable fit. This central stellar object contains less than 10% of the total light in the object, and may be indicative of an AGN. This galaxy, however, is not detected in the Chandra Deep Field South 2-Megasecond Catalog (Luo et al. 2008) nor in the radio VLA maps by Kellermann et al. (2008) and Miller et al. (2008). Figure 2 also shows that the inner part of the light profile of galaxy # 23495 ($r \lesssim 1''$) is barely resolved in all bands, suggesting another AGN. This appears confirmed by the fact that the galaxy is also detected in the Chandra image, and it has X-ray luminosity $3.8 \pm 0.24 \times 10^{43}$ erg/s and $5.6 \pm 0.6 \times 10^{43}$ erg/s in the soft and hard band, respectively; it is not, however, detected in the VLA maps.

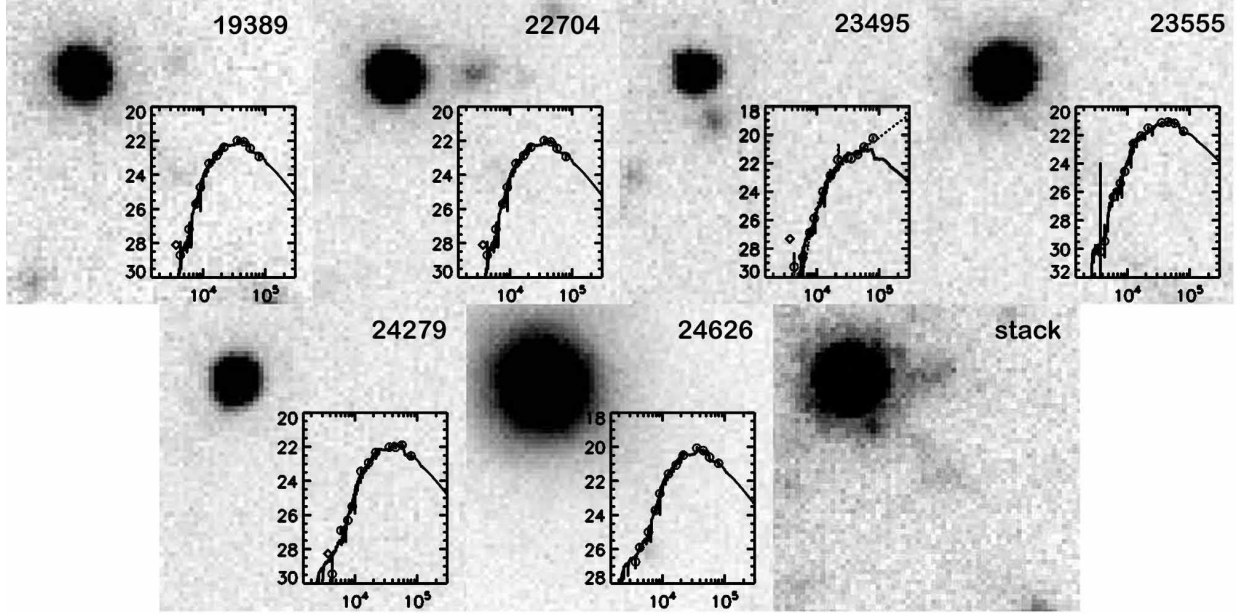


FIG. 1.— The H-band images of the sample galaxies, and the stacked image of all but galaxy # 23495. The size of each panel is $\sim 3.5 \times 3.5 \text{ arcsec}^2$. The insets show the observed (data points) and best-fit (curve) SED for each galaxy. For object # 23495 we also show the AGN SED best-fit as a dashed curve (see text).

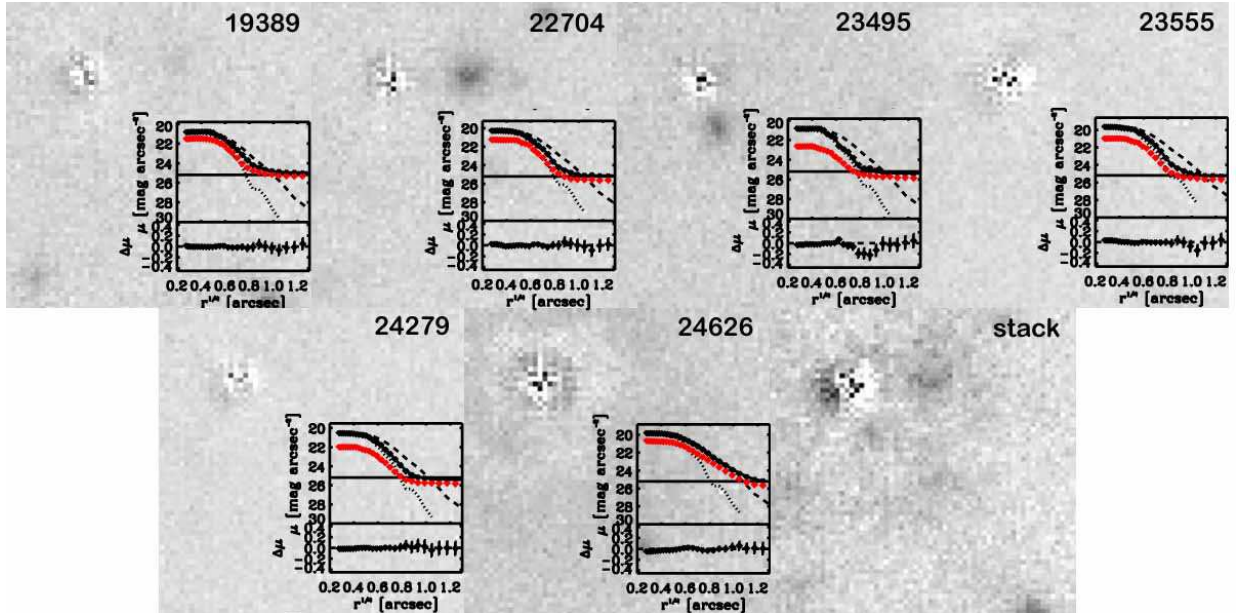


FIG. 2.— The H-band residual images of the sample galaxies and of the stacked image obtained subtracting the best-fit Sérsic model (after PSF convolution) from the original images. The insets show the observed profiles (diamonds), the best-fit profiles (continuous line), the psf profile (dotted line), a Sérsic model with $r_e = 3 \text{ kpc}$ and $n_{\text{Sérsic}} = 4$ (dashed line) and the residual profile (bottom panel). The sky level is shown as an horizontal line. Black symbols refer to the H-band light profile, red diamonds to the Y-band one. The red Y-H colors of our galaxies cause the Y-band profile to be always below the H-band one.

With the exception of the IRAC $8 \mu\text{m}$ data point, whose value suggests the presence of a hot dust component, the broad-band SED of this source is otherwise very similar to that of the other galaxies, and fits made under the assumption that its luminosity is powered by stars yield “stellar populations parameters” that are essentially the same as the other galaxies (see Table 1). We also note that fitting the SED of this galaxy with the AGN template by Polletta et al. (2006) returns the same value of

the photometric redshift as with stellar templates.

Galaxy # 24279 has a Sérsic index of intermediate value $n \sim 1.6$, suggesting that this is probably a bulge dominated disk galaxy. We note that Stockton et al. (2008) and McGrath et al. (2008) have found that some passive galaxies at $z > 1.5$ have disk morphology. Finally, to obtain a reasonable fit to the light profile of galaxy # 24626, we had to use a combination of two components: one with a very high Sérsic

TABLE 1
THE SAMPLE OF PASSIVE GALAXIES

ID	RA	DEC	$z^{(1)}$	$\log(M/M_{\odot})$	$\log(\text{SSFR})$ [Gyr $^{-1}$]	E(B-V)	Age	τ Gyr	Sérsic H -band	r_e [kpc]
19389	53.135730	-27.784932	1.307p	10.41	-5.55	0.1	3	0.2	2.99 ⁽²⁾	1.02 ⁽²⁾
22704	53.153799	-27.774587	1.384s	10.70	-5.55	0.15	3	0.2	2.65	0.50
23495	53.158455	-27.773982	2.349p	11.14	-3.39	0.15	2	0.2	⁽³⁾	< 0.38
23555	53.158810	-27.797155	1.921s	10.82	-2.98	0.0	2	0.2	1.97	0.44
24279	53.163005	-27.797655	1.980s	10.63	-3.39	0.15	3	0.5	1.63	0.37
24626	53.165159	-27.785869	1.317s	11.10	-2.11	0.1	3	0.5	7.42	3.69

NOTE. — (1): s and p indicate spectroscopic and photometric redshift, respectively; (2) modeled with the Sérsic profile plus the psf one; (3) modeled with the psf profile, so the size reported here is just an upper limit.

index to reproduce the inner part of the galaxy, and a second with $n \sim 1$ to reproduce the outskirts. Furthermore, both components have effective radius $r_e \sim 3$ kpc, implying that even if the component with lower surface brightness were not detected (e.g. in shallower images), the effective radius would still be found to be ~ 3 kpc, significantly larger than the other galaxies. Cases like this galaxy, therefore, do not provide an explanation to the much smaller size of the $z \sim 2$ ellipticals compared to those at $z \sim 0$.

We have also analyzed the residual maps produced by subtracting the best-fit models from the corresponding original images to investigate the presence of diffuse low-surface brightness halos, as recently suggested by some (Mancini et al. 2009; Hopkins et al. 2009b). For all galaxies, these maps (see Fig. 2) show the presence of residual structure in the innermost $0.5''$ of the light profile, where the contribution by the PSF is the largest. This is very likely the result of the variations of the PSF across the field, which cannot be taken into account by our average PSF. To verify this possibility we have fitted the individual stars using the same average PSF used for galaxies, and indeed we have found residuals similar in intensity and morphology to those of the galaxies. There is, however, no evidence of a halo. The only exception is the case of galaxy # 24626, which requires a two-component model to reproduce its light profile, an inner bulge and an outer disk. Subtracting both of these two components, however, leaves a complex residual map, revealing a substantially more irregular light distribution than the other galaxies.

To further explore the possible presence of a halo, we have stacked all the individual images together, except galaxy # 24626. In the H -band the stacked image has an equivalent exposure time $T_{exp} = 78,500$ sec and reaches 1σ surface brightness sensitivity $\mu_{H,stack} \sim 27$ mag arcsec $^{-2}$, and we have performed the GALFIT analysis on it following the same procedure used for individual galaxies. The stacked images and the GALFIT residuals are shown in Figures 1 and 2, respectively. Close companions were not masked before stacking and were not included in the GALFIT model. The stacked image, like the individual galaxies, is very compact. The residual images for individual galaxies and the stack show no evidence of a large-scale diffuse halo with less than 2% of the residual light falling within $2''$ of the source.

We plot in Figure 3 the Sérsic index (top) and effective radius (bottom) of the galaxies measured from the z , Y , J and H -band images as a function of wavelength. Assuming a mean redshift $\langle z \rangle = 1.7$ for the sample, the covered rest-frame wavelength range extends

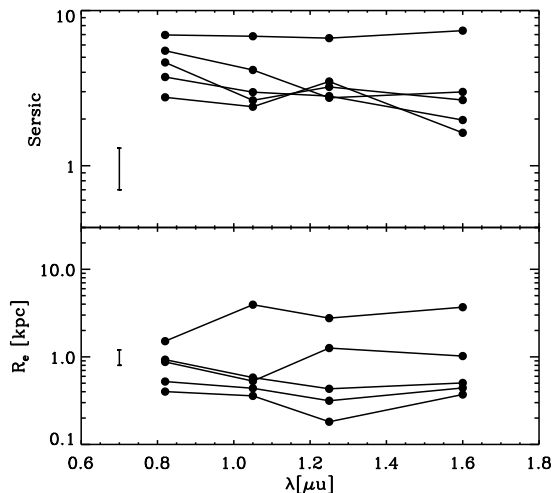


FIG. 3.— The Sérsic index (*upper panel*) and the effective radius (*bottom panel*) as a function of the wavelength. Object # 23495, the one best-fitted by a point like source, is not shown in this figure. The typical error bar is marked with a vertical bar, and amounts to $\sim 30\%$ of the measured Sérsic indices and $\sim 20\%$ of r_e .

from the rest-frame UV at $\lambda \sim 3300$ Å to the optical at $\lambda \sim 6000$ Å. Consistent with a visual inspection, the two plots show weak or no morphological k -correction. The Sérsic index is constant with wavelength within the errors, while the effective radius of three galaxies has a weak, but statistically significant dependence on it, decreasing by about $\sim 40\%$ from the z band to the H one (r_e is constant for the remainder of the sample). This weak dependence of r_e with wavelength results in a negative color gradient, with the outer parts of the galaxies being bluer than the center. This color gradient has also been observed by Guo et al. (in preparation), who report that SED fitting implies that the stellar populations in the outer regions of these galaxies are, on average, younger by ≈ 0.5 Gyr than those in the center. Finally, we note that the observed weak dependence of morphology on wavelength is in good quantitative agreement with other studies of early-type galaxies at high-redshift from ACS and NICMOS images (McCarthy et al. 2007; Trujillo et al. 2007) as well as at lower redshift (Pavovich et al. 2003; Cassata et al. 2005).

4. THE MASS-SIZE RELATION AT $Z \sim 2$

In Figure 4 we compare the relationship between stellar mass and size in the H band for the six galaxies in

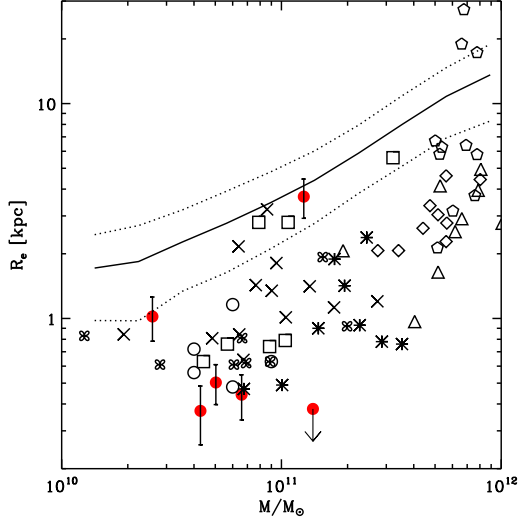


FIG. 4.— The effective radius as a function of stellar mass for early-type galaxies. Our sample is marked with red filled circles, with galaxy # 23495 shown as an upper limit, since it is unresolved. Crosses, circles, clovers, squares, stars, triangles, pentagons and diamonds represent the galaxies from Cimatti et al. (2008), Zirm et al. (2007), Toft et al. (2007), Daddi et al. (2005), Van Dokkum et al. (2008), Trujillo et al. (2006), Mancini et al. (2009) and Longhetti et al. (2007), respectively. The continuous and dashed lines represent the local relation and its $1-\sigma$ scatter, from Shen et al. (2003).

our sample to other measures from the literature, both at high redshift and in the local universe. When needed, we have homogenized mass measures to M05 and CB07 with Salpeter IMF by applying offsets¹¹ computed by Salimbeni et al. (2009). The figure shows that four out of our six galaxies are located below the local relation for early-type galaxies. The remaining two galaxies (#19389 and #24626) are on the local relation.

Thus, on the one hand our small sample of ~ 2 massive and passive galaxies seems to confirm that a significant fraction of these systems are ~ 3 to 5 times smaller, and hence have ~ 50 – 100 times denser central stellar density, than their local counterparts, as previously reported from similar but shallower and/or lower quality images (Trujillo et al. 2007; Toft et al. 2007; Zirm et al. 2007; Longhetti et al. 2007; Van Dokkum et al. 2008; Toft et al. 2009) or at UV rest-frame wavelengths (Daddi et al. 2005; Cimatti et al. 2008). On the other hand, it also suggests a diversity of morphological properties (size and stellar mass density) among these galaxies, with some of them being similar to the local ones, which still remains to be characterized from a statistical point of view. We plan to report soon on one such study.

5. SUMMARY AND CONCLUSIONS

Massive galaxies ($M \sim 10^{11} M_\odot$) with early spectral type at $z \sim 2$ appear to often have a relatively smooth and regular morphology, nearly independent of the wavelength, and with light profile which is well described by a Sérsic model, i.e. their morphology can be classified as “elliptical”, although systems with an exponential component are also observed. This suggests that a tight cor-

relation between spectral and morphological properties similar to what is observed in the local universe, i.e. the back bone of the Hubble sequence, is already in place among bright galaxies at $\sim 25\%$ of the cosmic time. The Sérsic analysis has also quantitatively shown that the morphology of these galaxies depends very mildly on the wavelength, between the rest-frame UV and optical windows.

One of our six galaxies is almost certainly an AGN, while another with a spatially unresolved nuclear component is a candidate one. Such kind of contamination should not be surprising given the similarity between the SED of obscured AGN and quiescent galaxies. By the same token, however, it is also possible that both types of sources contribute to the luminous output of the same galaxy, a fact that we have not directly investigated in this work. The apparently high level of contamination (33% of our sample) observed at $z \sim 2$, the cosmic era when both AGN and star-formation activity both reach their maximum (Ueda et al. 2003), raises the intriguing question of whether this is direct evidence of a link between the AGN and the mechanisms responsible for the cessation of star formation in the galaxies. We plan to report on this issue using larger samples from imminent new observations with WFC3 of the GOODS fields. The high AGN contamination is also likely to bias statistical conclusions made from UV/Optically-selected samples of passive galaxies at $z \sim 2$, unless sensitive X-ray and mid-IR photometry (Daddi et al. 2005, 2007), or at least multi-wavelength high-resolution *HST* imaging, can be used (like in the GOODS) to cull these sources. In surveys where such information is not available, like some recent ground-based ones (e.g. van Dokkum et al. 2009), the AGN so frequently encountered among the galaxies cannot be recognized.

Four out of six of our $z \sim 2$ ellipticals lie below the local mass-size relation for early-type galaxies, in agreement with previous findings that they can be up to ~ 3 – 5 times more compact at given mass, and thus ~ 30 – 100 times denser, than their local counterparts. Of the remaining two galaxies, however, one (#19389), which has an unresolved central component, is at the boundary of the local relation, while the other (#24626) is well within it. We have not found any evidence of a low-surface brightness halo surrounding these galaxies, either in the individual images, or in their stacked one. At most, only $< 2\%$ of the light (and hence of the mass, assuming a constant M/L ratio) can be segregated in such a halo. Galaxy #24626, requires a two-component light profile, one Sérsic model with high n (spheroid) embedded in a disk, to provide a good fit to the observations, but both have the same, relatively large, effective radius, $r_e \sim 3$ kpc. Thus, what is emerging here is that these galaxies are characterized by a dispersion of properties that also includes systems similar to the local ones, as some have already suggested (Cimatti et al. 2008; Mancini et al. 2009), which however still needs to be studied and characterized. Until this work is done, whether and/or how the ultra-compact $z \sim 2$ ellipticals evolve into the local ones or whether ultra-compact systems are also present in the local universe but have so far eluded detection will remain open questions.

¹¹ $\log(M_{CB07,M05}) = \log(M_{BC03}) - 0.2$ and $\log(M_{Salp}) = \log(M_{Chab}) + 0.25$

We acknowledge the anonymous referee for the useful comments. PC acknowledges support from NASA grant HST-GO-09822.45-A.

REFERENCES

- Arnouts, S. et al. 2007, *A&A*, 476, 137
 Beckwith, S. V. W. et al. 2006, *AJ*, 132, 1729
 Buitrago, F., et al. 2008, *ApJ*, 687, 61L
 Bundy, K., et al. 2006, *ApJ*, 651, 120
 Calzetti, D., et al. 2000, *ApJ*, 533, 682
 Cassata, P., et al. 2005, *A&A*, 357, 903
 Cimatti, A., et al. 2008, *A&A*, 482, 21
 Daddi, E., et al. 2004, *ApJ*, 617, 746
 Daddi, E., et al. 2005, *ApJ*, 626, 680
 Daddi, E., et al. 2007, *ApJ*, 670, 163
 Fontana, A., et al. 2006, *A&A*, 459, 745
 Fontana, A., et al. 2009, *A&A*, 501, 15
 Giavalisco, M., et al. 2004, *ApJ*, 600, L93
 Hopkins, P. F., et al. 2009, *MNRAS*, 401, 1099
 Hopkins, P. F., et al. 2009, *MNRAS*, 398, 898
 Ilbert, O., et al. 2009, *ApJ*, 709, 644
 Kellermann, K. I., et al. 2008, *ApJS*, 179, 71
 Kormendy, J., et al. 2009, *ApJS*, 182, 216
 Laidler, V. G., et al. 2007, *PASP*, 119, 1325
 Longhetti, M., et al. 2007, *MNRAS*, 374, 614
 Luo, B., et al. 2008, *ApJS*, 179, 19
 Maraston, C., 2005, *MNRAS*, 362, 799
 McGrath, E. J., et al. 2008, *ApJ*, 682, 303
 Mancini, C., et al. 2009, *MNRAS*, 401, 933
 Miller, N. A., et al. 2008, *ApJS*, 179, 114
 Naab, T., et al. 2009, *ApJ*, 690, 1452
 Papovich, C., et al. 2003, *ApJ*, 598, 827
 Peng, C. Y., et al. 2002, *AJ*, 124, 266
 Polletta, M., et al. 2006, *ApJ*, 642, 673
 Ravindranath, S., et al. 2006, *ApJ*, 652, 963
 Renzini, A., 2006, *ARA&A*, 44, 141
 Salimbeni, S., et al. 2009, *American Institute of Physics Conference Series*, Vol. 1111, 207
 Scarlata, C., et al. 2007, *ApJS*, 172, 494
 Shen, S., et al. 2003, *MNRAS*, 343, 978
 Stockton, A., et al. 2008, *ApJ*, 672, 146
 Stoughton, C., et al. 2002, *AJ*, 123, 485
 Toft, S., et al. 2007, *ApJ*, 671, 285
 Toft, S., et al. 2009, *ApJ*, 705, 255
 Trujillo, I., et al. 2006, *MNRAS*, 373, L36
 Trujillo, I., et al. 2007, *MNRAS*, 382, 109
 Ueda, Y., et al. 2003, *ApJ*, 598, 886
 Van Dokkum, P. G., et al. 2008, *ApJ*, 677, L5
 Van Dokkum, P. G., et al. 2009, *PASP*, 121, 2
 Valentinuzzi, T., et al. 2009, [astro-ph/0907-2392]
 Vanzella, E., et al. 2008, *A&A*, 478, 83
 Zirm, A. W., et al. 2007, *ApJ*, 656, 66